Supporting Information

for

A Terminally Protected Dipeptide: from Crystal Structure and Self-Assembly, through Co-Assembly with Carbon-Based Materials, to a Ternary Catalyst for Reduction Chemistry in Water

*Daniela Mazzier, Francesco Carraro, Marco Crisma, Marzio Rancan, Claudio Toniolo, and Alessandro Moretto**

D. Mazzier, F. Carraro, Dr. M. Rancan, Prof. C. Toniolo, Prof. A. Moretto
Department of Chemical Sciences, University of Padova, 35131 Padova, Italy
E-mail: alessandro.moretto.1@unipd.it
Dr. M. Rancan
Institute for Energetics and Interphases, CNR, 35131 Padova, Italy
Dr. M. Crisma, Prof. C. Toniolo, Prof. A. Moretto
Institute of Biomolecular Chemistry, Padova Unit, CNR, 35131 Padova, Italy

*Address correspondence to: alessandro.moretto.1@unipd.it

CONTENTS

GENERAL METHODS

NMR

^{1}H and ^{13}C NMR spectra were recorded at room temperature on a Bruker AC-200 (200 MHz) instrument using the partially deuterated solvent as the internal reference. Chemical shifts (δ) are expressed in ppm. The multiplicity of a signal is indicated as: br - broad, s - singlet, d - doublet, t - triplet, m - multiplet, etc.

Mass Spectrometry

ESI-MS experiments were performed using an ESI-ToF Mariner™ Biospectrometry™ Workstation of Applied Biosystems by flow injection analysis using MeOH as the mobile phase. High-resolution mass spectra were obtained by electrospray ionization on a Perseptive Biosystem Mariner ESI-ToF spectrometer (Foster City, CA). An 1 x 10^{-9} M solution of neurotensin, angiotensin I, and bradykinin in an 1:1 CH_3CN/H_2O mixture, containing 1% formic acid, was used for calibration.

Transmission electron microscopy (TEM)

Samples were analyzed on a Jeol 300PX instrument. Samples were prepared immediately before used. A small drop of solutions was floated on a glow discharged carbon coated grid and excess was removed by #50 hardened Whatman filter paper. For the samples with negative staining, the grid was then floated on 2% uranyl acetate solution for 10 seconds, and the excess was removed by #50 hardened Whatman filter paper.

Scanning electron microscopy (SEM)

A Carl Zeiss Merlin field emission scanning electron microscope operating at 5kV accelerating voltage was used. A small drop of the milk-like aqueous suspension was placed on a microscope glass cover slip and allowed to dry overnight.

FT-IR absorption

FT-IR absorption spectra in KBr discs were recorded with a Perkin-Elmer 1720X spectrophotometer; ν_{max} is given for the main absorption bands.

SYNTHESES AND CHARACTERIZATIONS

General

1-hydroxy-7-aza-1,2,3-benzotriazole (HOAt) was purchased from GL Biochem (Shanghai) Ltd. H-Cys(Me)-OH, H-Leu-OMe·HCl, Boc-Leu-OH and N-(3-Dimethylaminopropyl)-N′-ethylcarbodiimide hydrochloride (EDC·HCl) were obtained from Iris Biotech (Germany). Di-tert-butyl dicarbonate (Boc_2O), thionyl chloride, propargylamine, 1,8-Diazabicyclo[5.4.0]undec-7-ene (DBU), Triethylamine (TEA), N,N,N′,N′-Tetramethylethylenediamine (TMEDA), copper(I) iodide and nickel(II) chloride hydrate were obtained from Sigma-Aldrich.
The deuterated solvent $CDCl_3$ was purchased from Euriso-Top (France).
All other chemicals and solvents were Sigma-Aldrich, Fluka or Acros products and used as provided without further purifications.

Synthesis of Boc-Cys(Me)-OH

H-Cys(Me)-OH (5 g, 367 mmol) was dissolved in 80 mL of solvent mixture of CH_3CN/H_2O (1:1 v/v) with TEA (6 mL, 43 mmol). Boc_2O (8.4 g, 38.4 mmol) was dissolved in 25 mL of CH_3CN and added to solution of amino acid. The mixture was stirred at rt for 18 h. The organic solvent was removed under reduced pressure and the aqueous residue was acidified with HCl 1M. The precipitate was extracted with AcOEt (3v), then the organic phase was washed with water (2v) and brine. The organic layer was dried over Na_2SO_4, filtered and evaporated to dryness under reduced pressure. The product was recovered as an oil (8.2 g, 94% yield).

HRMS (ESI+): *m/z* calcd. 235.0878, found 236.1029 $[M+H]^+$.

FT-IR absorption: ῡ 3318, 3103, 2979, 2924, 1716, 1510, 1394, 1368, 1249, 1164, 1056 cm^{-1}.

^1H NMR (200 MHz, $CDCl_3$) δ 7.60 (s br, 1H, COOH), 5.42 (d, 1H, NH urethane), 4.54 (d, 1H, αCH), 2.97 (d, 2H, βCH_2), 2.14 (s, 3H,), 1.44 (s, 9H, $3CH_3$ Boc).

^{13}C NMR (50 MHz, $CDCl_3$) δ 175.52, 155.70, 80.74, 53.02, 36.46, 28.42, 16.39.

Synthesis of Boc-Cys(Me)-Leu-OMe

Boc-Cys(Me)-OH (6.76 g, 28.7 mmol) was dissolved in CH_2Cl_2 and activated with HOAt (3.9 g, mmol) and EDC·HCl (5.48 g, mmol). Separately H-Leu-OMe·HCl was dissolved in CH_2Cl_2 with addition of TEA (8 mL, 57.5 mmol) and the obtained solution was added to the active ester. TEA (4 mL, mmol) was added to the resulting mixture until basic pH. The mixture was stirred at rt for 18 h. The solvent was removed under reduced pressure and the residue dissolved in AcOEt. The organic phase was washed with 5% $KHSO_{4(aq)}$ (4v), 5% $NaHCO_{3(aq)}$ (3v) and brine. The organic layer was dried over Na_2SO_4, filtered and evaporated under reduced pressure. The residue was dissolved in AcOEt and precipitated by addition of petroleum ether. After filtration and drying, the product was obtained as a white solid (8.35 g, 84% yield).

HRMS (ESI+): *m/z* calcd. 362.1875, found 363.1966 $[M+H]^+$.

FT-IR absorption: ῡ 3342, 3281, 3085, 2973, 2920, 1756, 1682, 1656, 1557, 1522, 1315, 1274, 1251, 1225, 1197, 1158, 1020 cm^{-1}.

^1H NMR (200 MHz, $CDCl_3$) δ 6.84 (d, 1H, NH amide), 5.37 (d, 1H, NH urethane), 4.66-4.55 (m, 1H, αCH), 4.30-4.20 (m, 1H, αCH), 3.73 (s, 3H, -OMe), 2.98-2.67 (m, 2H, βCH_2 Cys), 2.17 (s, 3H, -SMe), 1.68-1.60 (m, 3H, βCH_2 and γCH Leu), 1.46 (s, 9H, $3CH_3$ Boc), 0.93 (d, 6H, δCH_3 Leu).

^{13}C NMR (50 MHz, $CDCl_3$) δ 173.08, 170.68, 155.53, 80.65, 53.59, 52.46, 51.09, 41.63, 36.41, 28.40, 24.93, 22.92, 22.02, 16.04.

Synthesis of H-Cys(Me)-OMe·HCl

H-Cys(Me)-OH (5 g, 0.037 mmol) was suspended in 120 mL of dry MeOH and cooled in a MeOH/ice bath. Then $SOCl_2$ (10 mL) was added dropwise to the mixture. After removal of the bath, the mixture was refluxed for 2 days. The residual solid was removed by filtration and the filtered was evaporated under reduced pressure. The residue was dissolved in the minimal amount of MeOH and precipitated by addition of Et_2O. The solid recovered after filtration was dried obtaining 4.8 g of product as a solid (70% yield).

HRMS (ESI+): *m/z* calcd. 149.0510, found 150.3091 $[M+H]^+$.

FT-IR absorption: ῡ 3003, 2864, 2633, 2500, 1743, 1594, 1571, 1507, 1434, 1316, 1235, 1206, 1064 cm^{-1}.

^{1}H NMR (200 MHz, DMSO) δ 8.91 (s, 3H, NH_2·HCl), 4.23 (t, 1H, αCH), 3.74 (s, 3H, -OMe), 3.04 (d, 2H, βCH_2), 2.11 (s, 3H, -SMe).

^{13}C NMR (50 MHz, DMSO) δ 168.73, 52.82, 51.63, 33.37, 15.38.

Synthesis of Boc-Leu-Cys(Me)-OMe

Boc-Leu-OH (2 g, 8.65 mmol) was dissolved in 40 mL of CH_2Cl_2 and activated with HOAt (1.18 g, 8.67 mmol) and EDC·HCl (1.65 g, 8.64 mmol). Separately H-Cys(Me)-OMe·HCl (1.6 g, 8.62 mmol) was dissolved in CH_2Cl_2 with addition of TEA (2.4 mL, 10.7 mmol) and the obtained solution was added to the active ester. TEA was added to the resulting mixture until basic pH. The mixture was stirred at rt for 48 h. The solvent was removed under reduced pressure and the residue dissolved in AcOEt. The organic phase was washed with 5% $KHSO_{4(aq)}$ (4v), 5% $NaHCO_{3(aq)}$ (3v) and brine. The organic layer was dried over Na_2SO_4, filtered and evaporated under reduced pressure. The residue was dissolved in AcOEt and precipitated by addition of petroleum ether. After filtration and drying, the product was obtained as a white solid (2 g, 64 % yield).

HRMS (ESI+): *m/z* calcd. 362.1865, found 363.3309 $[M+H]^+$.

FT-IR absorption: ῡ 3325, 2955, 2921, 1747, 1740, 1689, 1649, 1525, 1443, 1276, 1208, 1169 cm^{-1}.

^{1}H NMR (200 MHz, $CDCl_3$) δ 6.88 (d, 1H, NH amide), 4.87 (d, 1H, NH urethane), 4.84-4.66 (m, 1H, αCH), 4.14 (d, 1H, αCH), 3.76 (s, 3H, -OMe), 2.95 (dd, 2H, βCH_2 Cys), 2.10 (s, 3H, -SMe), 1.77-1.56 (m, 3H, βCH_2 and γCH Leu), 1.44 (s, 9H, 3 CH_3 Boc), 0.94 (dd, 6H, δCH_3 Leu).

^{13}C NMR (50 MHz, $CDCl_3$) δ 172.60, 171.23, 155.70, 80.33, 53.21, 52.74, 51.78, 41.25, 36.45, 28.42, 24.84, 23.05, 22.06, 16.32.

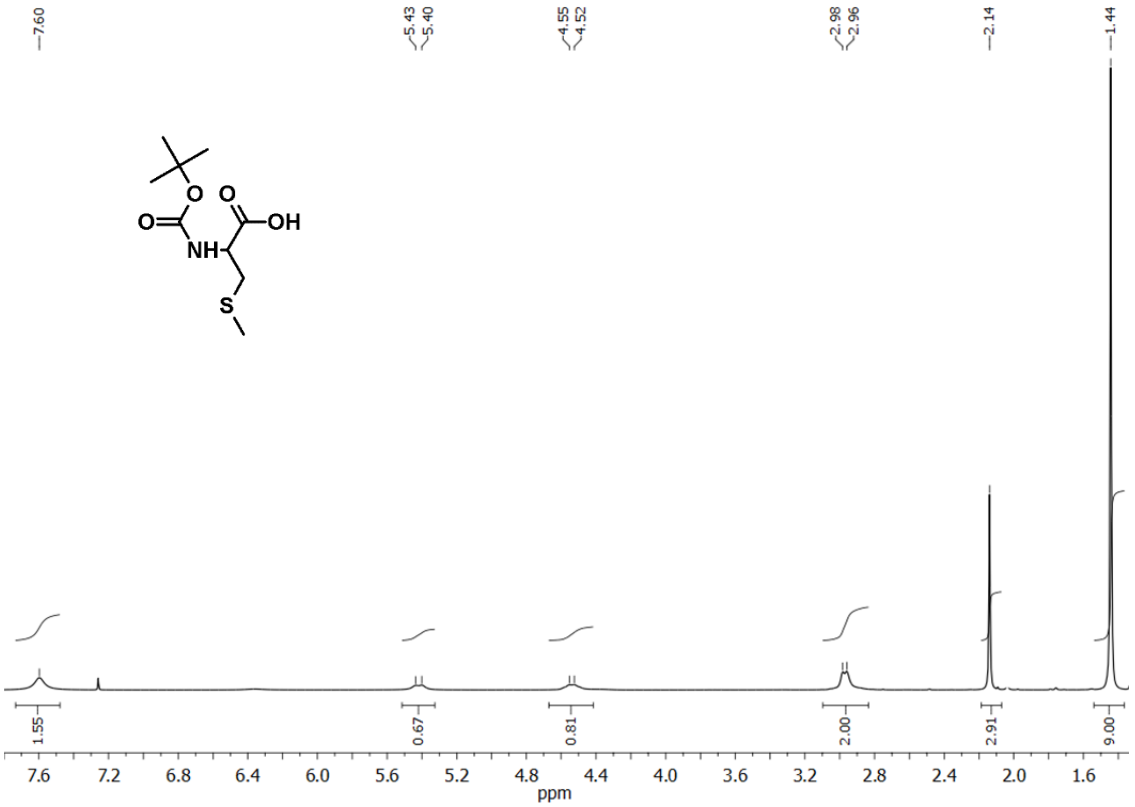

Fig. S1 ^{1}H NMR spectra of Boc-Cys(Me)-OH in $CDCl_3$.

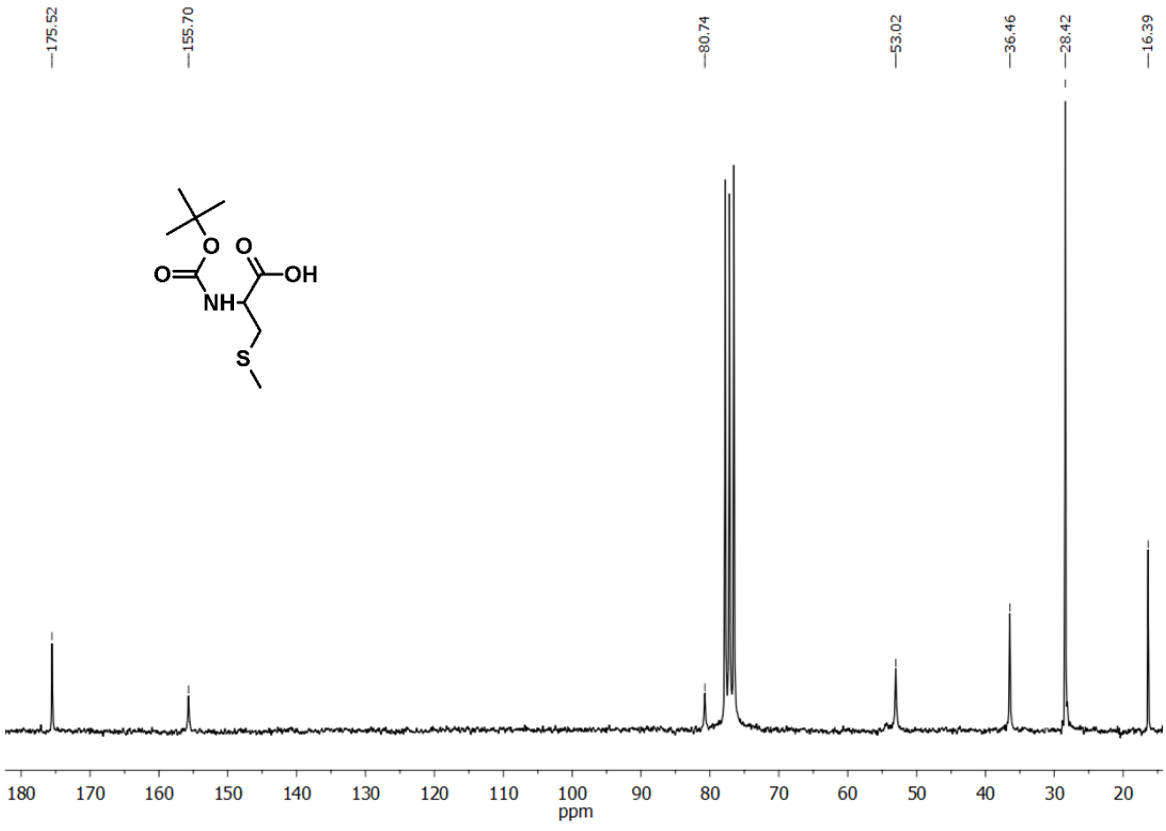

Fig. S2 ^{13}C NMR spectra of Boc-Cys(Me)-OH in $CDCl_3$.

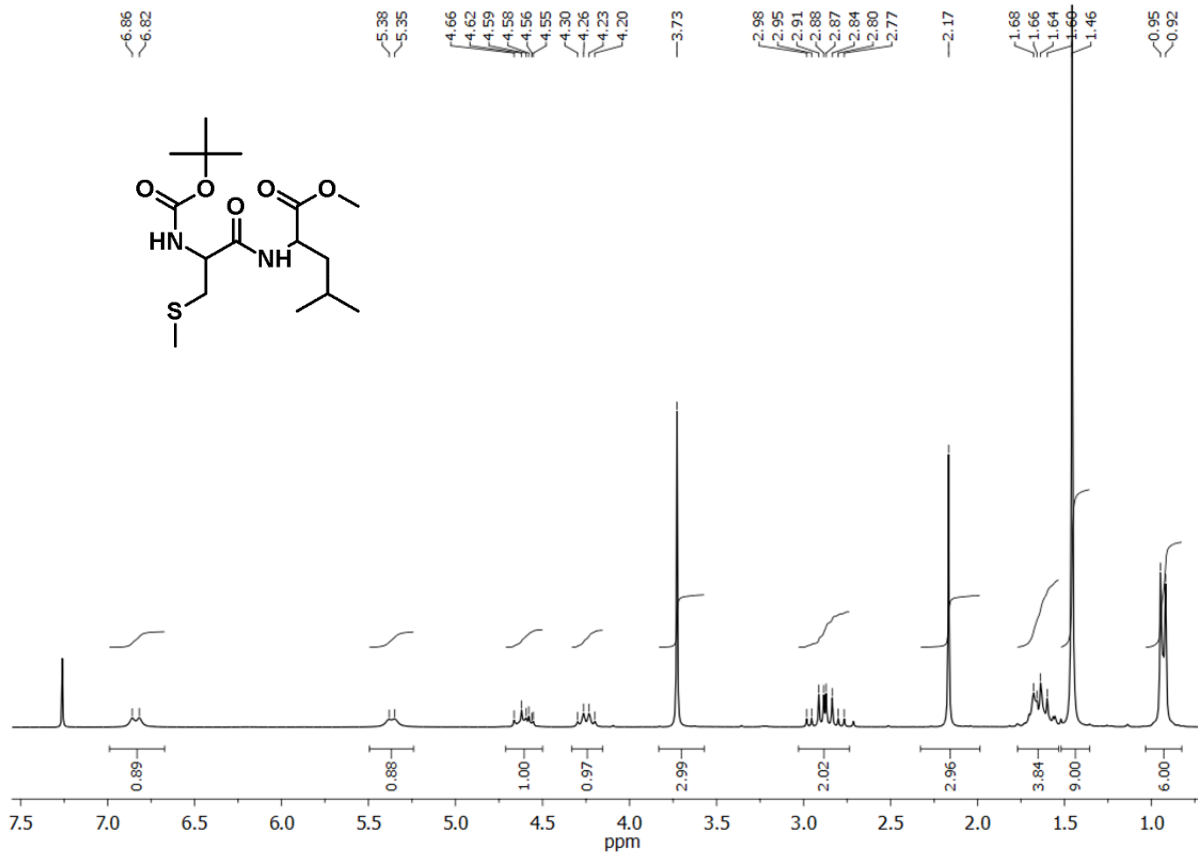

Fig. S3 ^{1}H NMR spectra of Boc-Cys(Me)-Leu-OMe in $CDCl_3$.

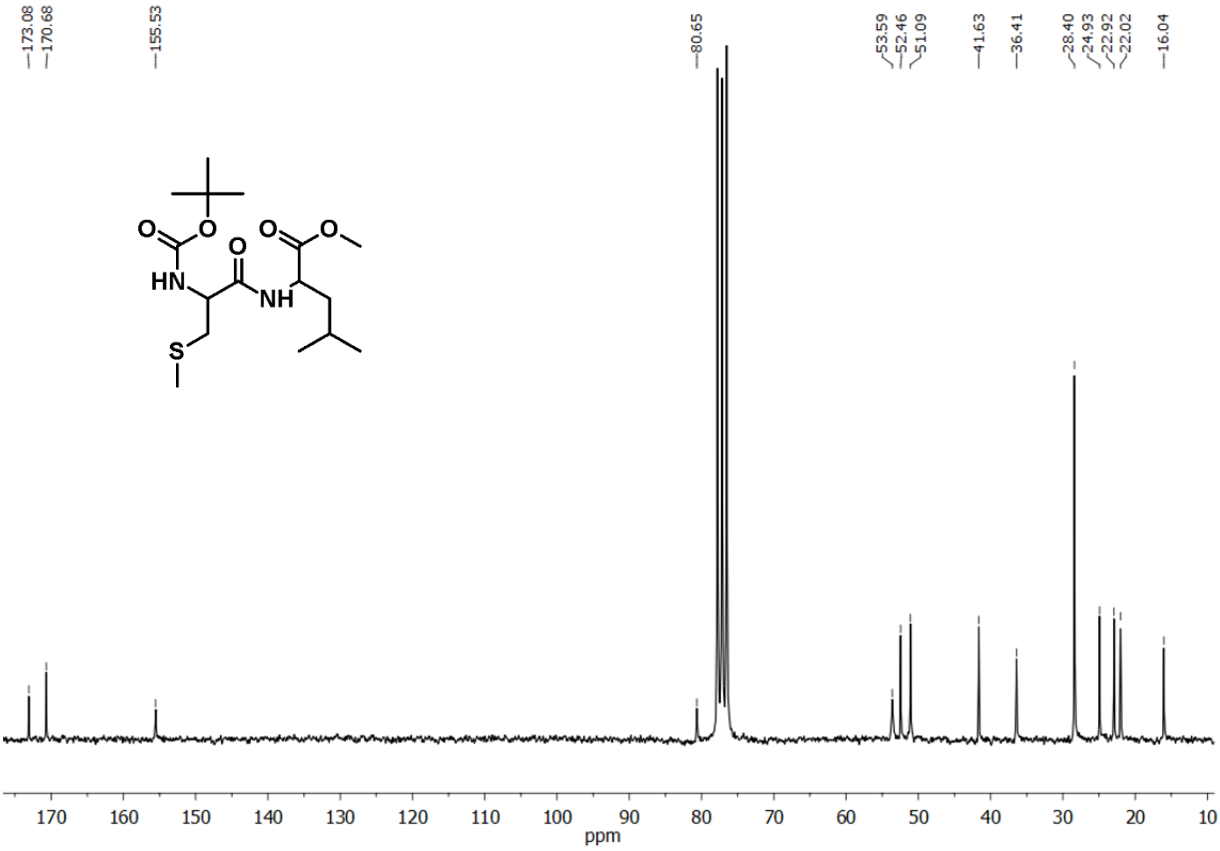

Fig. S4 ^{13}C NMR spectra of Boc-Cys(Me)-Leu-OMe in $CDCl_3$.

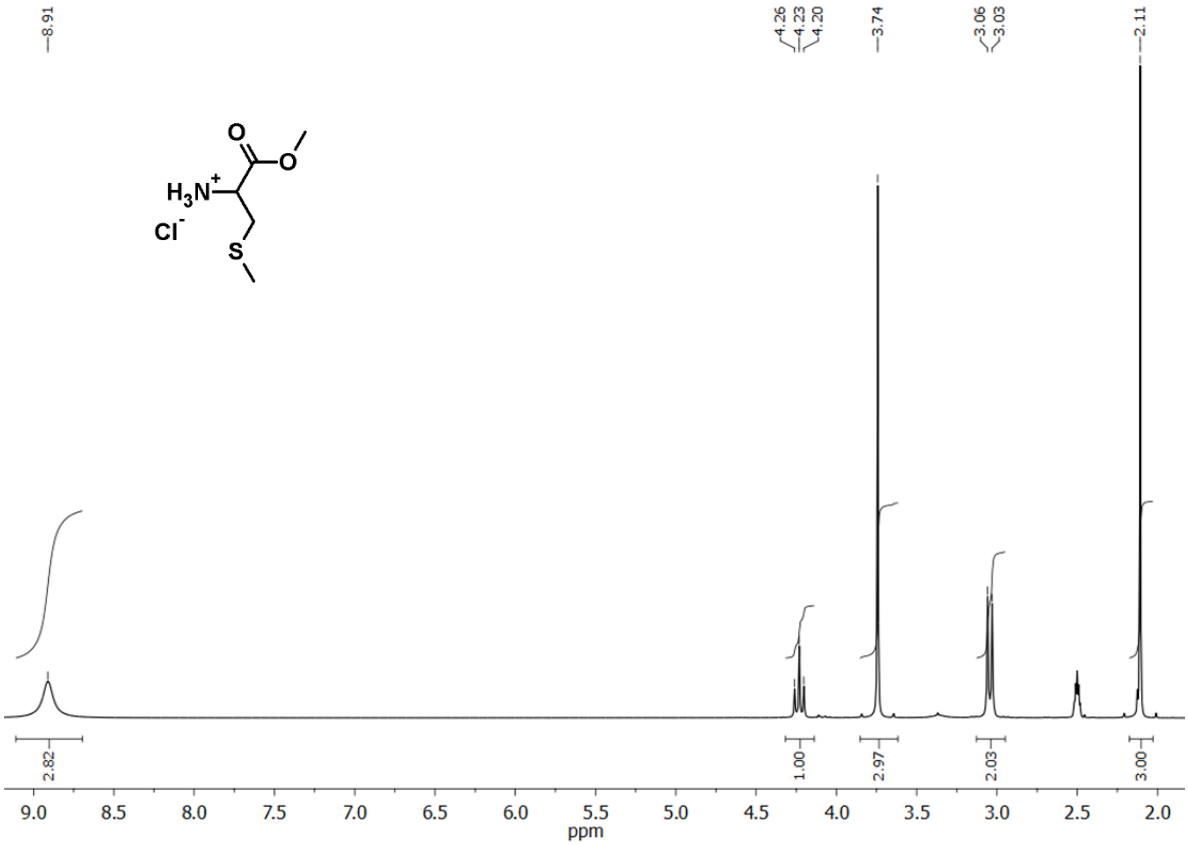

Fig. S5 ^{1}H NMR spectra of H-Cys(Me)-OMe·HCl in DMSO-d_6.

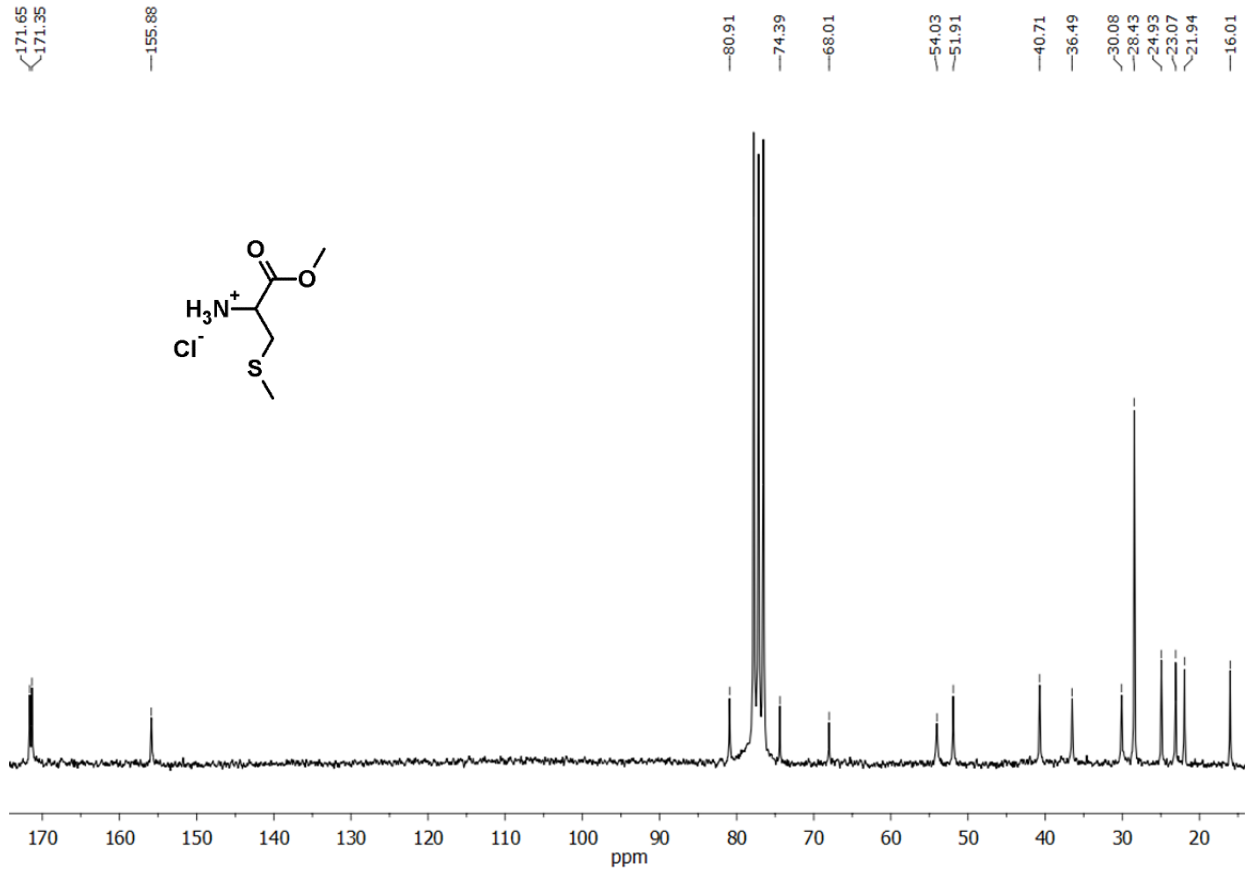

Fig. S6 ^{13}C NMR spectra of H-Cys(Me)-OMe·HCl in DMSO-d_6.

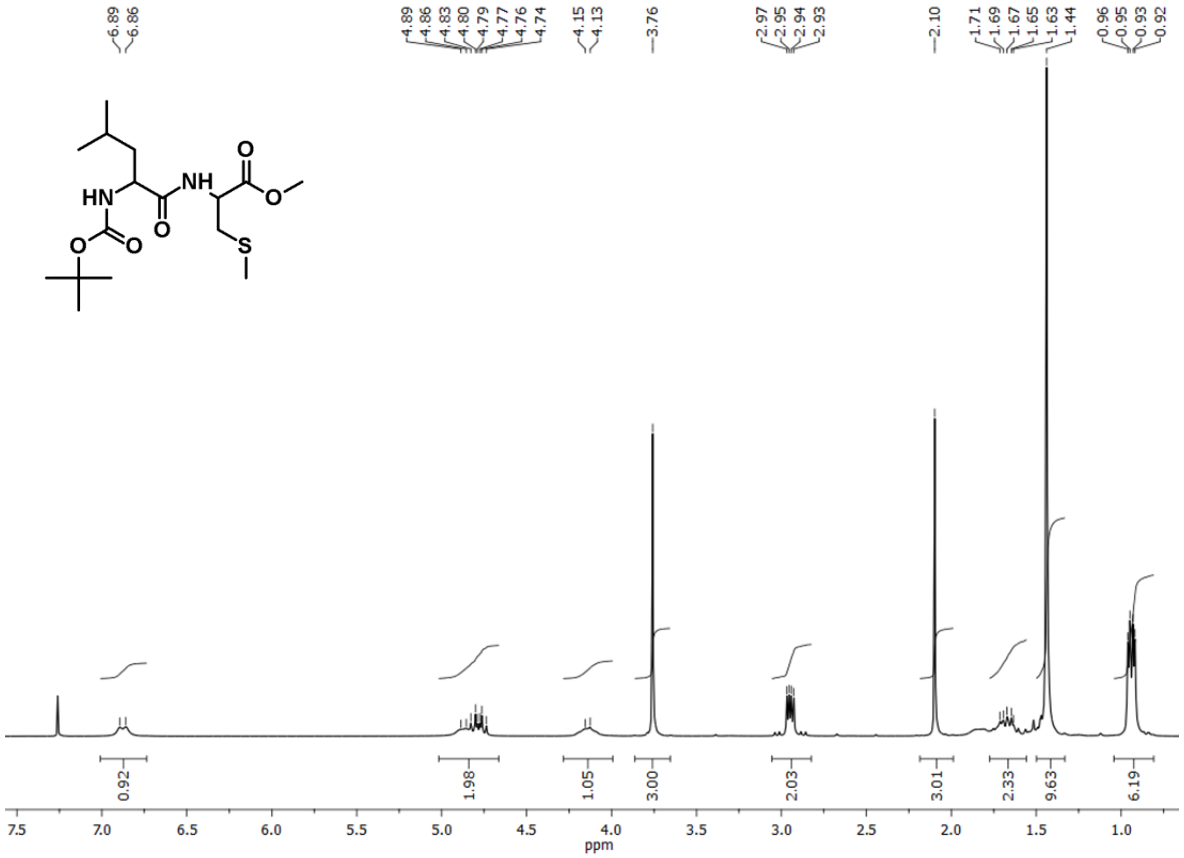

Fig. S7 ^{1}H NMR spectra of Boc-Leu-Cys(Me)-OMe in $CDCl_3$.

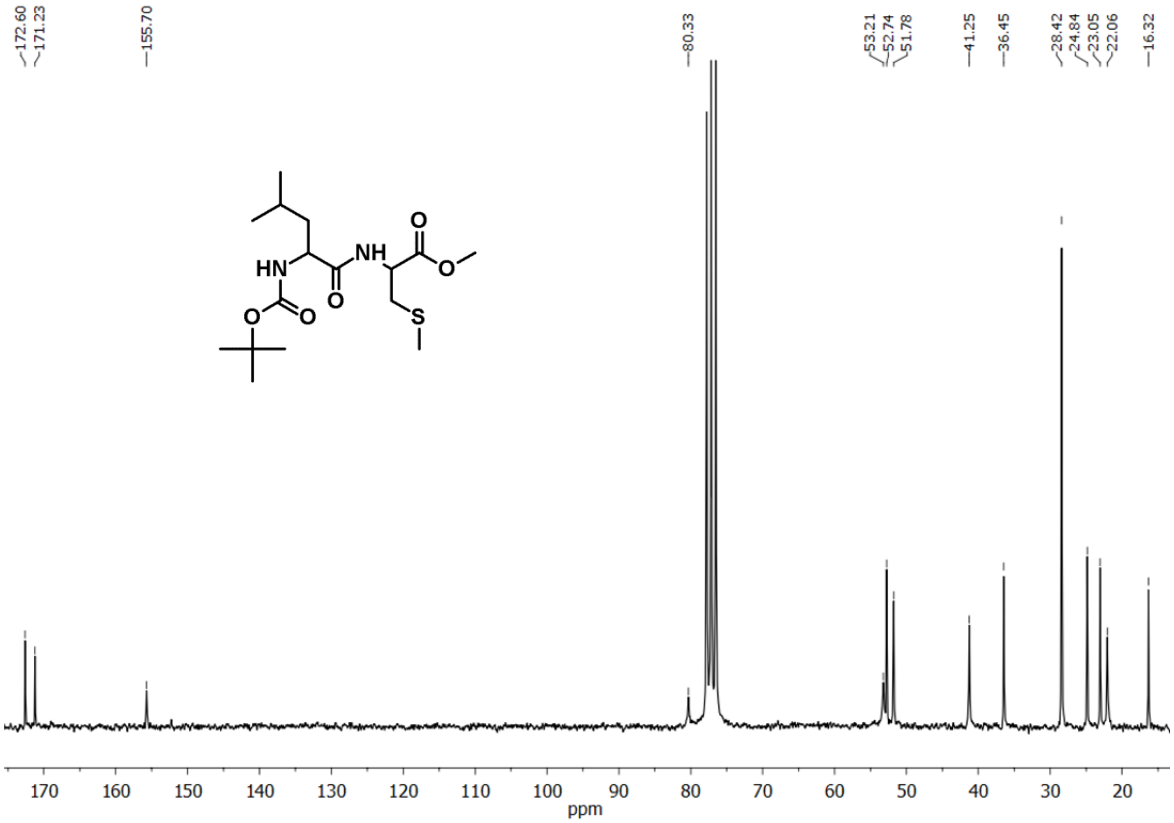

Fig. S8 ^{13}C NMR spectra of Boc-Leu-Cys(Me)-OMe in $CDCl_3$.

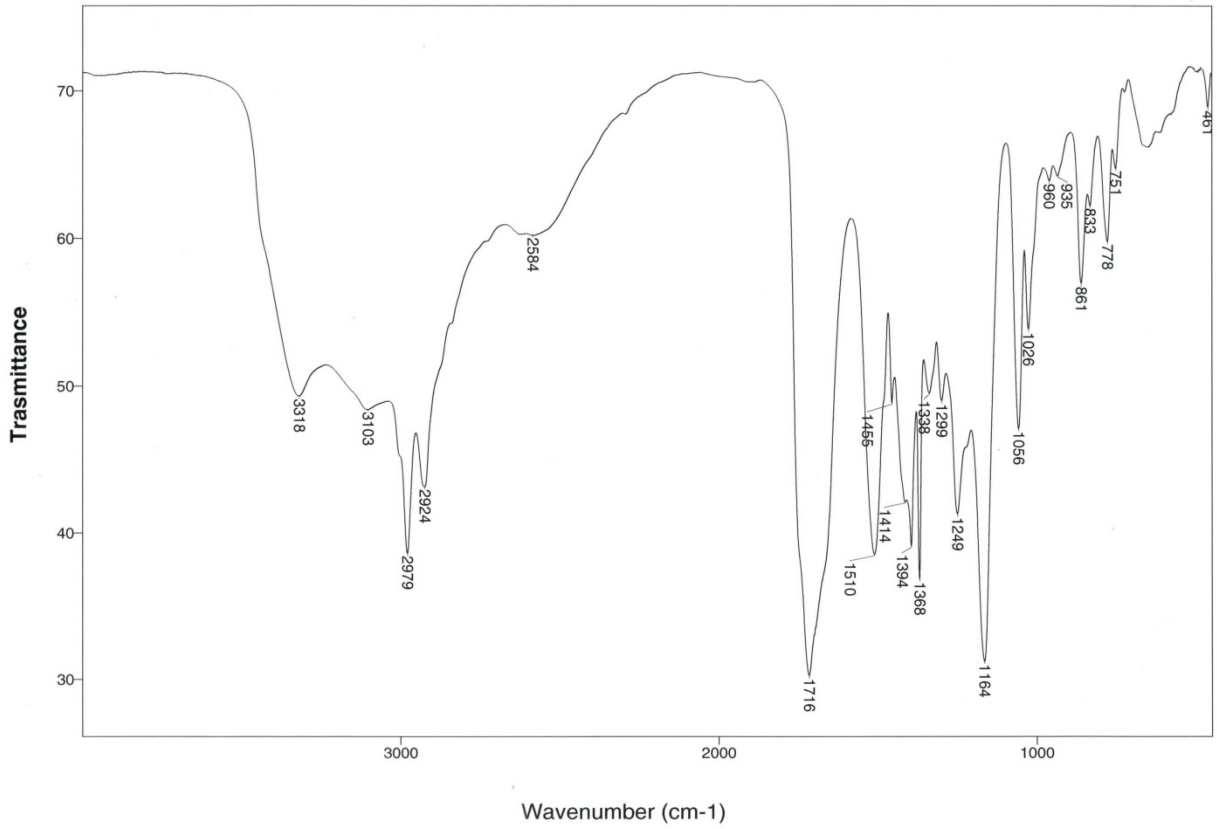

Fig. S9 FT-IR spectrum of Boc-Cys(Me)-OH in KBr disc.

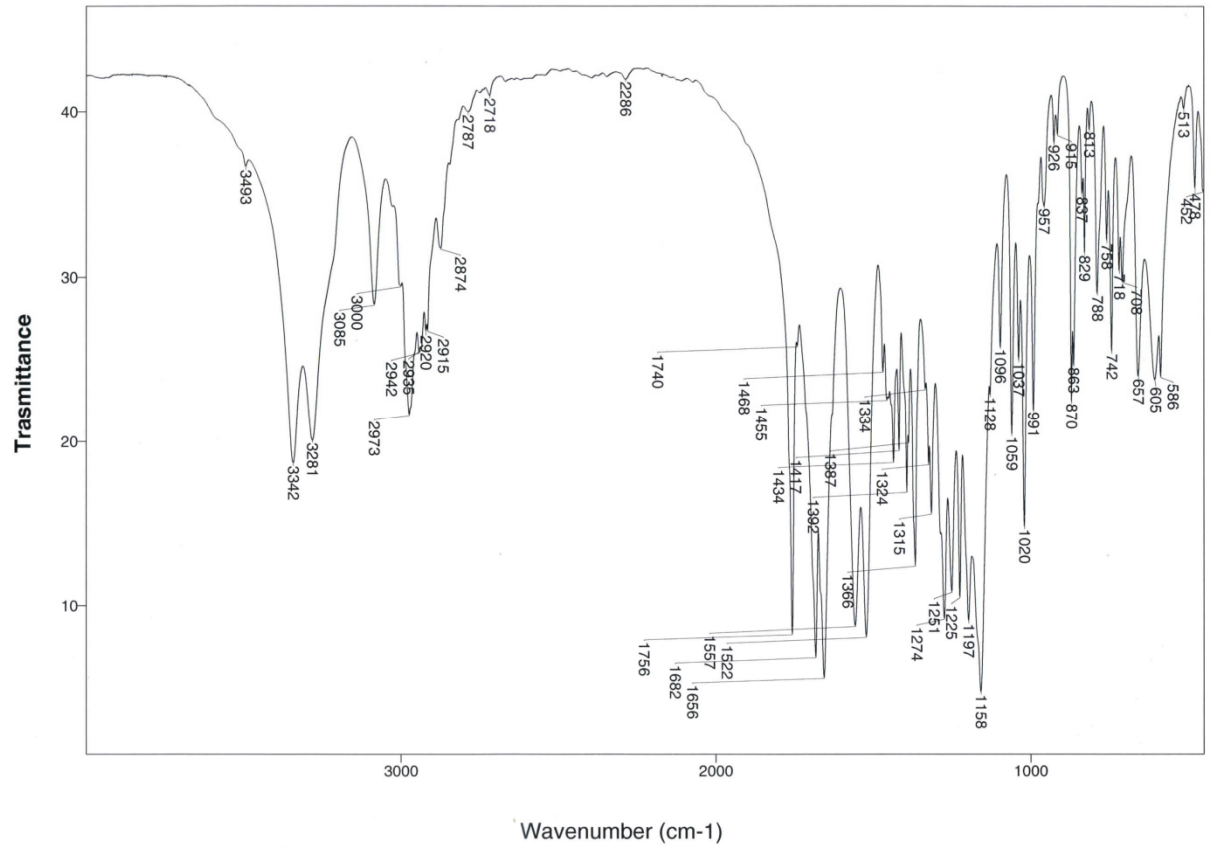

Fig. S10 FT-IR spectrum of Boc-Cys(Me)-Leu-OMe in KBr disc.

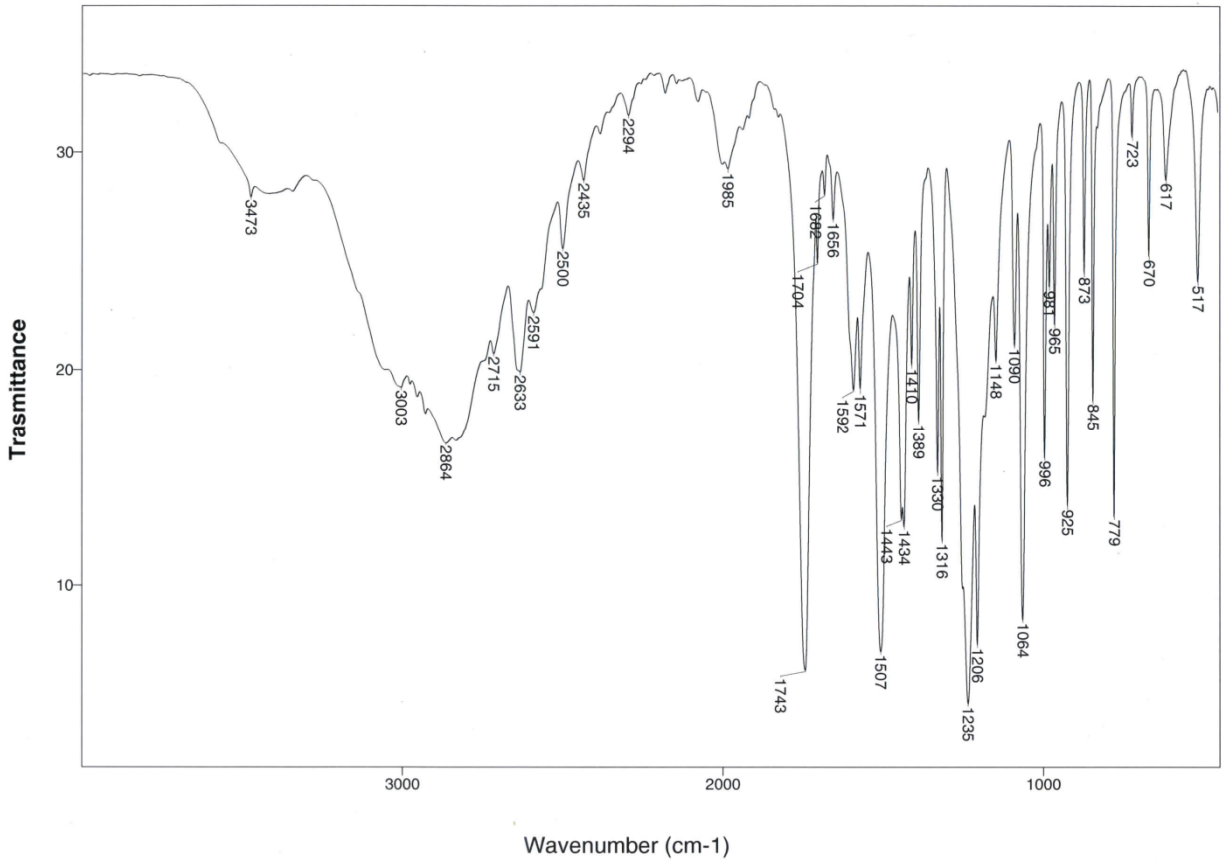

Fig. S11 FT-IR spectrum of H-Cys(Me)-OMe·HCl in KBr disc.

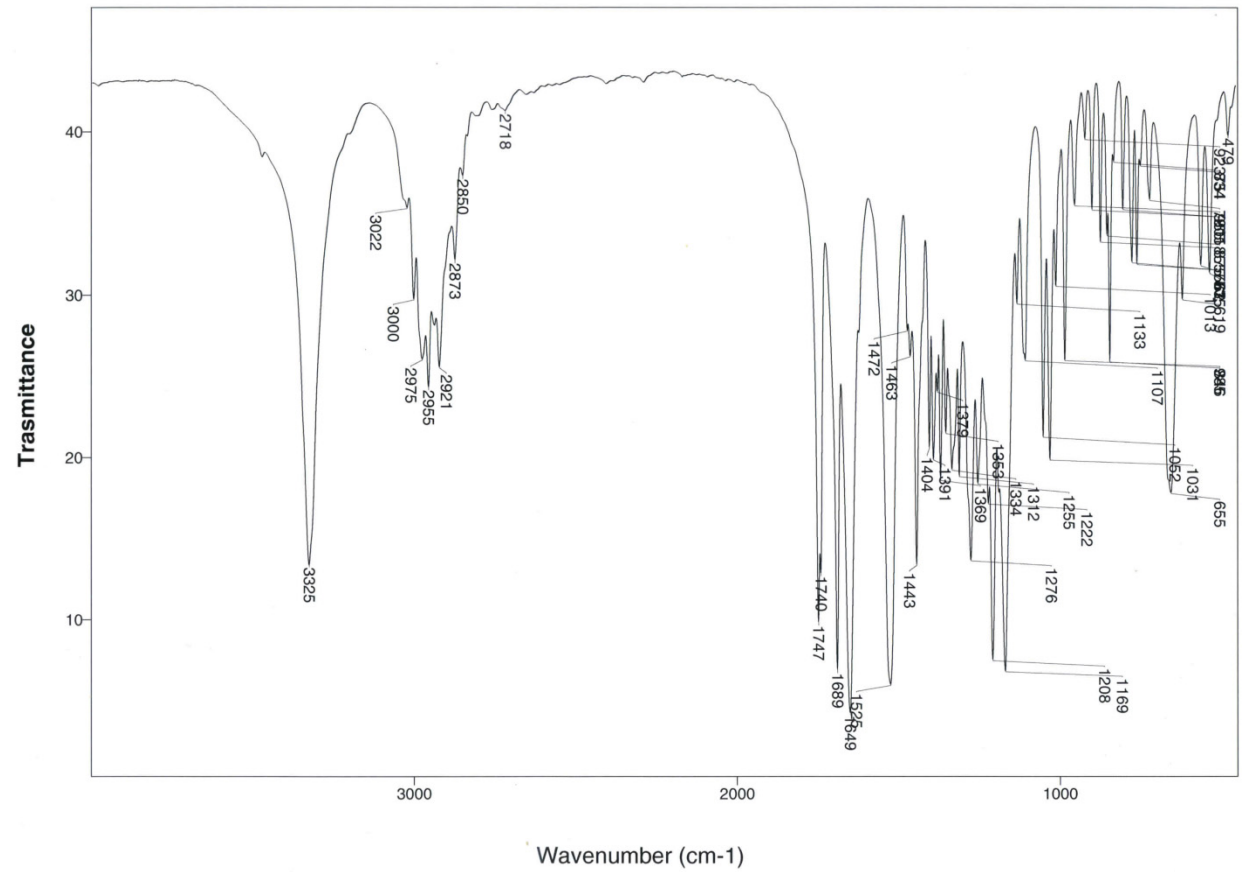

Fig. S12 FT-IR spectrum of Boc-Leu-Cys(Me)-OMe in KBr disc.

X-Ray diffraction

Crystals of Boc-L-Cys(Me)-L-Leu-OMe and Boc-L-Leu-L-Cys(Me)-OMe were grown by slow evaporation from methanol. X-Ray diffraction data were collected with an Agilent Technologies Gemini E four-circle kappa diffractometer equipped with a 92 mm EOS CCD detector, using graphite monochromated Cu Kα radiation (λ = 1.54178 Å). Data collection and reduction were performed with the CrysAlisPro software (version 1.171.36.28; Agilent Technologies). A semi-empirical absorption correction based on the multi-scan technique using spherical harmonics, implemented in the SCALE3 ABSPACK scaling algorithm, was applied.

Both structures were solved by ab initio procedures of the SIR 2002 program,[S1] and refined by full-matrix least-squares on F^2, using all data, by application of the SHELXL-97 program,[S2] with anisotropic displacement parameters for all of the non-H atoms. H-Atoms were calculated at idealized positions and refined using a riding model. Details specific to the individual structures are given below. Relevant crystal data and structure refinement parameters are listed in Tables S1 and S2. CCDC-1057628 and 1057629 contain the supplementary crystallographic data for this paper. These data can be obtained from The Cambridge Crystallographic Data Centre via www.ccdc.cam.ac.uk/data_request/cif.

Boc-L-Cys(Me)-L-Leu-OMe (**1**)

Data collection was performed up to theta = 51.25° as the crystal, owing to its size (smallest dimension 0.01 mm), did not significantly diffract beyond 1.0 Å resolution. The choice of the hexagonal space group $P6_5$, rather than its enantiomorph $P6_1$, was based on the known (L) configuration of the Cys and Leu residues used in the synthesis. Restraints were applied to the anisotropic displacement parameters of the methyl carbon atoms of the Boc and OMe protecting groups and the Cys(Me) residue, to approach isotropic behavior. Overall, many crystallographic parameters suffer from the far from optimal crystal size and quality. We are confident, however, that the basic conformational features of the molecule and its packing mode, as discussed in this work, are unambiguously established.

Boc-L-Leu-L-Cys(Me)-OMe (**2**)

The Leu side chain shows positional disorder. It was refined on two sets of positions (atoms C1G, C1D1, C1D2 for the first set, while C1G', C1D3, C1D4 for the second set) with refined population parameters of 0.658(8) and 0.342(8), respectively. Restraints were applied to the bond distances and bond angles involving atoms of the disordered parts, as well to their anisotropic displacement parameters.

Structure description

The molecular structure of Boc-L-Cys(Me)-L-Leu-OMe, as determined by single-crystal X-ray diffraction analysis, is illustrated in Fig. S14. Backbone and side-chain torsion angles are listed in Table S3, whereas the intermolecular H-bond parameters are reported in Table S4.

The urethane, peptide and ester bonds (ω torsion angles) are found in the usual *trans* disposition. The conformation adopted by both α-amino acid residues is *semi*-extended, with values of ϕ,ψ backbone torsion angles –95.2(4)°,+132.9(3)° for L-Cys and –66.3(4)°,+158.5(3)° for L-Leu. Overall, the backbone is bent at the level of the α-carbon of Cys, and the N-H groups of Cys and Leu point to opposite directions.

In the packing mode, the N1-H group is intermolecularly H-bonded to the (*y*, -*x*+*y*, *z*+1/6) symmetry equivalent of the (urethane carbonyl) O0 atom, and the N2-H group is H-bonded to the (*x*-*y*, *x*, *z*-1/6) symmetry equivalent of the (peptide) O1 atom (Table S3). As a result, H-bonded molecules wrap around the sixfold screw axis along the *c* direction, each molecule being connected to the next by two H-bonds. (Figure S15a). The left-handed, supramolecular sixfold helix thus generated is characterized by a very narrow internal lumen, about 2.5 Å in diameter (Figure S15b). The Cys(Me) and Leu side chains, as well as the N- and C-terminal *tert*-butyl and methyl ester groups of each molecule are located on the external surface. Each helical row of molecules is surrounded by six counterparts (Figure S16). Lateral stabilization between rows is provided, in addition to van der Waals interactions, by a C-H…O interaction taking place between the (Boc) C02-H02B group and the (*x*-1, *y*-1, *z*) symmetry equivalent of the (methyl ester) OT atom (Table S3).

In the X-ray diffraction structure of Boc-L-Leu-L-Cys(Me)-OMe (Figure S17), the backbone conformation is characterized by sets of ϕ,ψ torsion angles –116.68(18)°,+108.45(17)° for L-Leu, and –159.11(15)°, –172.42(16)° for L-Cys. The most striking conformational difference between this peptide and its positional isomer Boc-L-Cys(Me)-L-Leu-OMe, described above, is found at the level of the C-terminal residue, which adopts an extended conformation in Boc-L-Leu-L-Cys(Me)-OMe while it is *semi*-extended in Boc-L-Cys(Me)-L-Leu-OMe.

The packing mode of Boc-L-Leu-L-Cys(Me)-OMe is characterized by the occurrence of two intermolecular H-bonds, namely between the N1-H group and the (*x*+1, *y*, *z*) translational equivalent of the (urethane carbonyl) O0 atom, and between the N2-H group and the (*x*-1, *y*, *z*) translational equivalent of the (peptide) O1 atom. Although the H-bond donor and acceptor atoms are the same as in the intermolecular H-bonding scheme of Boc-L-Cys(Me)-L-Leu-OMe, the

different symmetry operators involved result in a completely different overall packing arrangement. Indeed, at variance with the helical packing of Boc-L-Cys(Me)-L-Leu-OMe, the packing mode of Boc-L-Leu-L-Cys(Me)-OMe can be described as a highly corrugated arrangement of molecules in the *bc* plane, with the intermolecular H-bonds connecting molecules along the *a* direction (Figure S18).

Crystallographic references

[S1] M.C. Burla, M. Camalli, B. Carrozzini, G.L. Cascarano, C. Giacovazzo, G. Polidori, R. Spagna, *J. Appl. Crystallogr.* **2003**, *36*, 1103.

[S2] G.M. Sheldrick, *Acta Crystallogr.* **2008**, *A64*, 112-122.

Table S1. Crystal data and structure refinement for Boc-L-Cys(Me)-L-Leu-OMe.

Identification code	mc237f	
Empirical formula	$C_{16}H_{30}N_2O_5S$	
Formula weight	362.48	
Temperature	293(2) K	
Wavelength	1.54178 Å	
Crystal system	Hexagonal	
Space group	P 6_5	
Unit cell dimensions	a = 11.4458(2) Å	α= 90°.
	b = 11.4458(2) Å	β= 90°.
	c = 27.7551(5) Å	γ = 120°.
Volume	3148.95(10) $Å^3$	
Z	6	
Density (calculated)	1.147 Mg/m^3	
Absorption coefficient	1.580 mm^{-1}	
F(000)	1176	
Crystal size	0.20 × 0.05 × 0.01 mm^3	
Theta range for data collection	4.46 to 51.25°.	
Index ranges	$-11 \le h \le 11$, $-11 \le k \le 11$, $-27 \le l \le 27$	
Reflections collected	18290	
Independent reflections	2281 [R(int) = 0.0441]	
Completeness to theta = 51.25°	100.0 %	
Absorption correction	Semi-empirical from equivalents	
Max. and min. transmission	1.00000 and 0.81551	
Refinement method	Full-matrix least-squares on F^2	
Data / restraints / parameters	2281 / 31 / 217	
Goodness-of-fit on F^2	1.042	
Final R indices [I>2sigma(I)]	R_1 = 0.0403, wR_2 = 0.1040	
R indices (all data)	R_1 = 0.0468, wR_2 = 0.1083	
Absolute structure parameter	-0.01(3)	
Largest diff. peak and hole	0.307 and -0.145 e.$Å^{-3}$	

Table S2. Crystal data and structure refinement for Boc-L-Leu-L-Cys(Me)-OMe

Identification code	mc238f	
Empirical formula	$C_{16}H_{30}N_2O_5S$	
Formula weight	362.48	
Temperature	293(2) K	
Wavelength	1.54178 Å	
Crystal system	Orthorhombic	
Space group	$P2_12_12_1$	
Unit cell dimensions	a = 5.08911(7) Å	α= 90°.
	b = 12.09583(13) Å	β= 90°.
	c = 32.4406(4) Å	γ = 90°.
Volume	1996.95(4) Å^3	
Z	4	
Density (calculated)	1.206 Mg/m^3	
Absorption coefficient	1.661 mm^{-1}	
F(000)	784	
Crystal size	0.80 × 0.06 × 0.02 mm^3	
Theta range for data collection	2.72 to 69.34°.	
Index ranges	$-5 \le h \le 4$, $-14 \le k \le 14$, $-39 \le l \le 38$	
Reflections collected	14108	
Independent reflections	3652 [R(int) = 0.0220]	
Completeness to theta = 69.34°	98.1 %	
Absorption correction	Semi-empirical from equivalents	
Max. and min. transmission	1.00000 and 0.63618	
Refinement method	Full-matrix least-squares on F^2	
Data / restraints / parameters	3652 / 50 / 245	
Goodness-of-fit on F^2	1.035	
Final R indices [I>2sigma(I)]	R_1 = 0.0391, wR_2 = 0.1077	
R indices (all data)	R_1 = 0.0406, wR_2 = 0.1091	
Absolute structure parameter	0.00(2)	
Largest diff. peak and hole	0.280 and -0.173 e.Å^{-3}	

Table S3. Selected backbone and side-chain torsion angles [°] for Boc-L-Cys(Me)-L-Leu-OMe and Boc-L-Leu-L-Cys(Me)-OMe.

Boc-L-Cys(Me)-L-Leu-OMe			Boc-L-Leu-L-Cys(Me)-OMe		
Torsion angle			Torsion angle		
C01-OU-C0-N1	θ^1	179.0(3)	C01-OU-C0-N1	θ^1	-179.00(18)
OU-C0-N1-C1A	ω_0	-175.2(3)	OU-C0-N1-C1A	ω_0	-179.10(15)
C0-N1-C1A-C1	ϕ_1	-95.2(4)	C0-N1-C1A-C1	ϕ_1	-116.68(18)
N1-C1A-C1-N2	ψ_1	132.9(3)	N1-C1A-C1-N2	ψ_1	108.45(17)
C1A-C1-N2-C2A	ω_1	171.1(3)	C1A-C1-N2-C2A	ω_1	-173.14(15)
C1-N2-C2A-C2	ϕ_2	-66.3(4)	C1-N2-C2A-C2	ϕ_2	-159.11(15)
N2-C2A-C2-OT	ψ_2	158.5(3)	N2-C2A-C2-OT	ψ_2	-172.42(16)
C2A-C2-OT-CT	ω_T	176.6(5)	C2A-C2-OT-CT	ω_T	176.39(19
N1-C1A-C1B-S1	χ_1^1	-73.8(4)	N1-C1A-C1B-C1G	χ_1^1	-82.1(3) / -51.0(4)[a]
C1A-C1B-S1-C1D	χ_1^2	-74.4(4)	C1A-C1B-C1G-C1D1	$\chi_1^{2,1}$	65.9(5) / -58.7(9)[b]
N2-C2A-C2B-C2G	χ_2^1	-72.8(4)	C1A-C1B-C1G-C1D2	$\chi_1^{2,2}$	-171.3(3) / 178.5(6)[c]
C2A-C2B-C2G-C2D1	$\chi_2^{2,1}$	163.0(3)	N2-C2A-C2B-S2	χ_2^1	71.18(19)
C2A-C2B-C2G-C2D2	$\chi_2^{2,2}$	-74.7(4)	C2A-C2B-S2-C2D	χ_2^2	-80.84(18)

[a] Minor occupancy conformer N1-C1A-C1B-C1G'.

[b] Minor occupancy conformer C1A-C1B-C1G'-C1D3.

[c] Minor occupancy conformer C1A-C1B-C1G'-C1D4.

Table S4. Hydrogen bond parameters [Å and °] for Boc-L-Cys(Me)-L-Leu-OMe.

D-H...A	d(D-H)	d(H...A)	d(D...A)	<(DHA)
N1-H1...O0#1	0.86	2.09	2.929(4)	164
N2-H2...O1#2	0.86	2.01	2.868(4)	179
C02-H02B…OT#3	0.96	2.54	3.485(5)	168

Symmetry transformations used to generate equivalent atoms:

#1: y,-x+y,z+1/6; #2: x-y,x,z-1/6; #3: x-1, y-1, z

Table S5. Hydrogen bond parameters [Å and °] for Boc-L-Leu-L-Cys(Me)-OMe.

D-H...A	d(D-H)	d(H...A)	d(D...A)	<(DHA)
N1-H1...O0#1	0.86	2.12	2.965(2)	166.7
N2-H2...O1#2	0.86	2.25	3.093(2)	167.1

Symmetry transformations used to generate equivalent atoms:

#1: x+1,y,z; #2: x-1,y,z

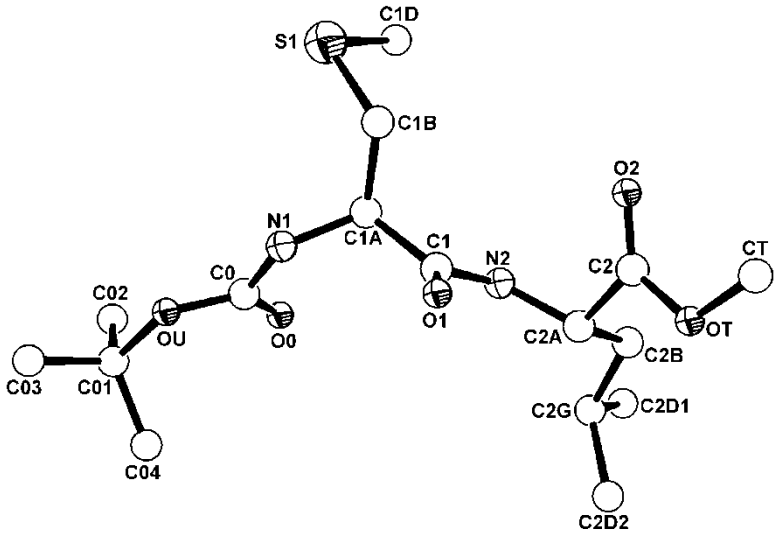

Fig. S13. X-Ray diffraction structure of Boc-L-Cys(Me)-L-Leu-OMe with atom numbering.

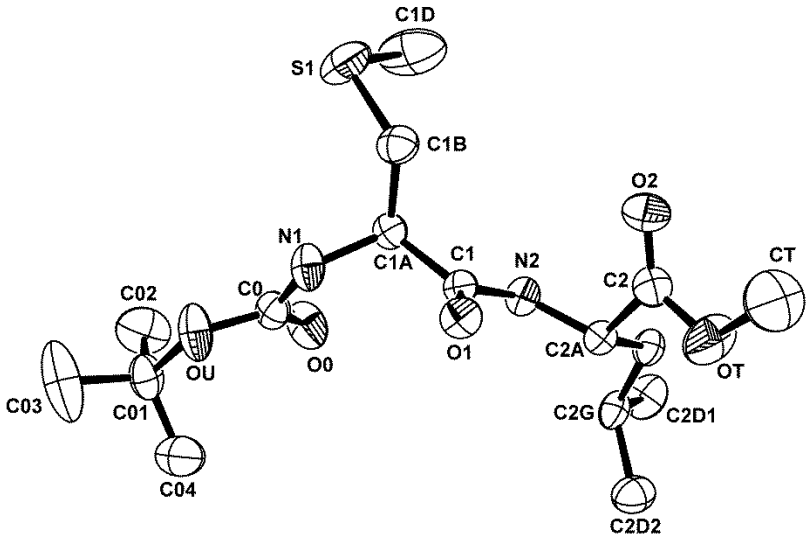

Fig. S14. X-Ray diffraction structure of Boc-L-Cys(Me)-L-Leu-OMe with atom numbering. Anisotropic displacement ellipsoids are drawn at the 30% probability level

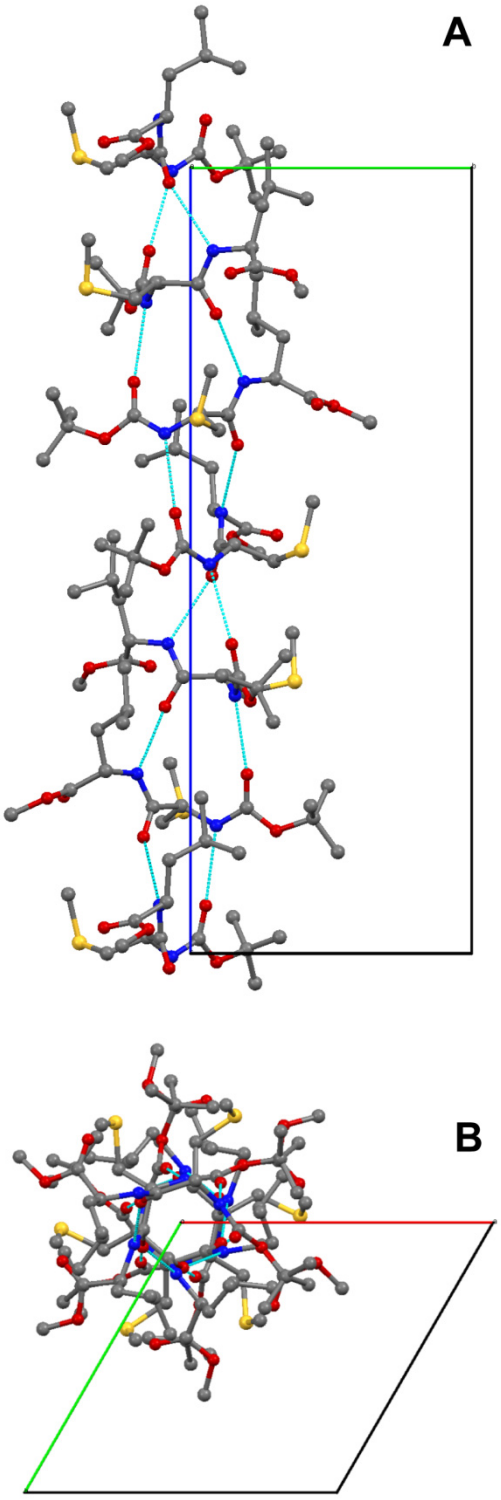

Figure S15. Packing mode of Boc-L-Cys(Me)-L-Leu-OMe. A single helical row of molecules is shown as viewed (**a**) perpendicularly and (**b**) down the sixfold screw axis. Intermolecular H-bonds are indicated by dashed lines.

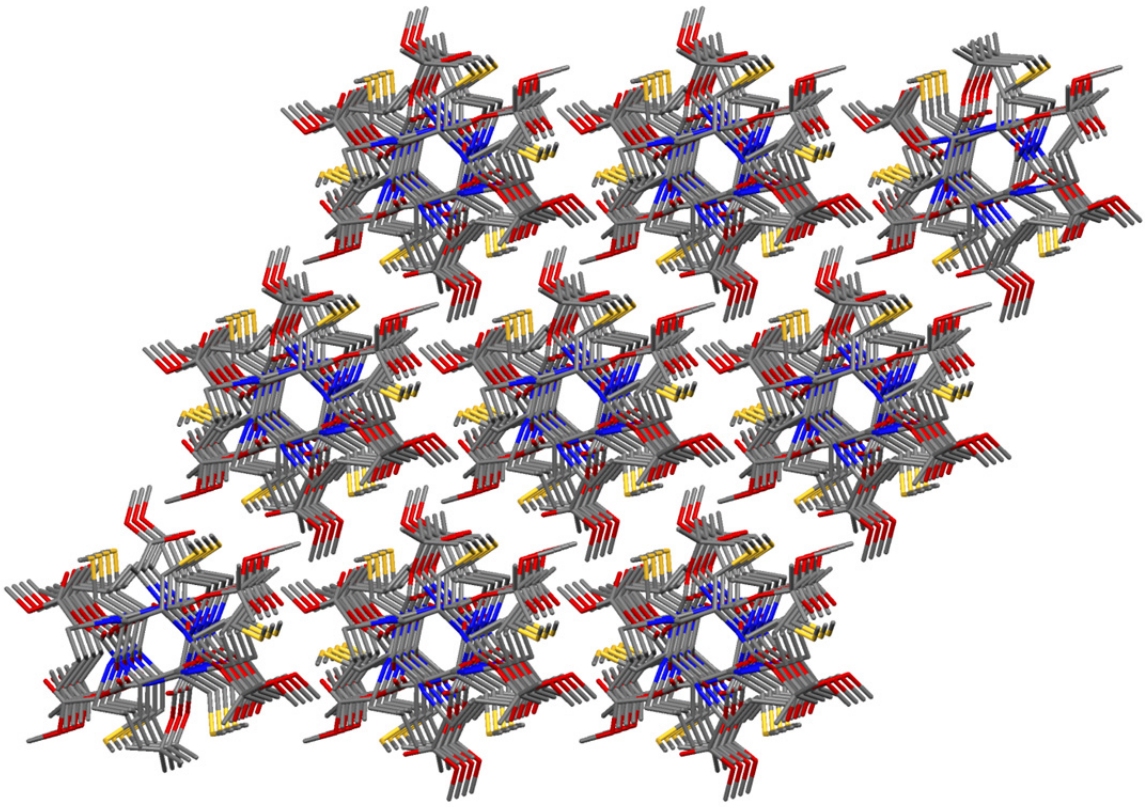

Figure S16. Overall packing of Boc-L-Cys(Me)-L-Leu-OMe as viewed nearly down the *c* axis.

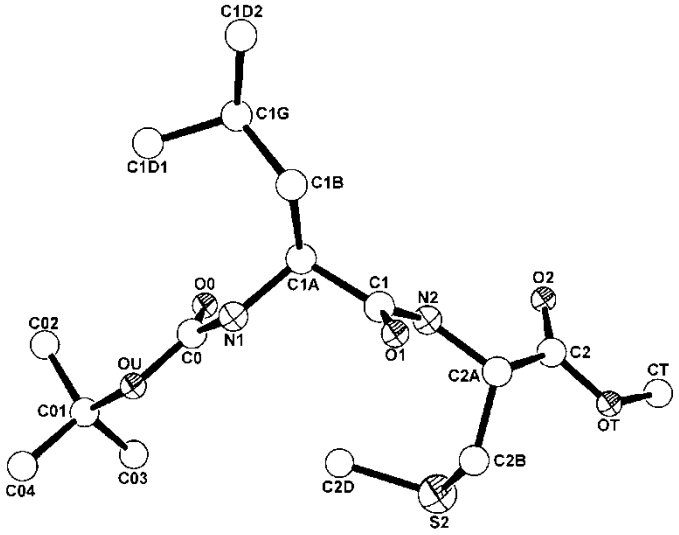

Figure S17. X-Ray diffraction structure of Boc-L-Leu-L-Cys(Me)-OMe with atom numbering. Only the major occupancy site for the disordered Leu side chain is shown.

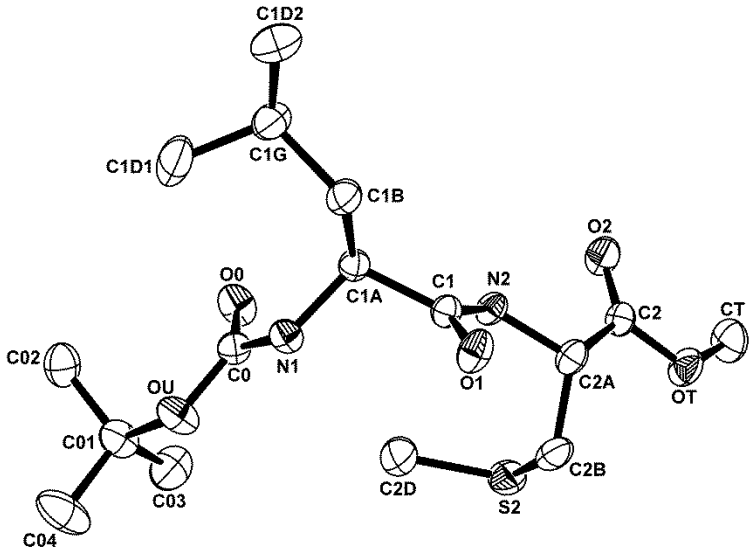

Fig. S18. X-Ray diffraction structure of Boc-L-Leu-L-Cys(Me)-OMe with atom numbering. Anisotropic displacement ellipsoids are drawn at the 30% probability level

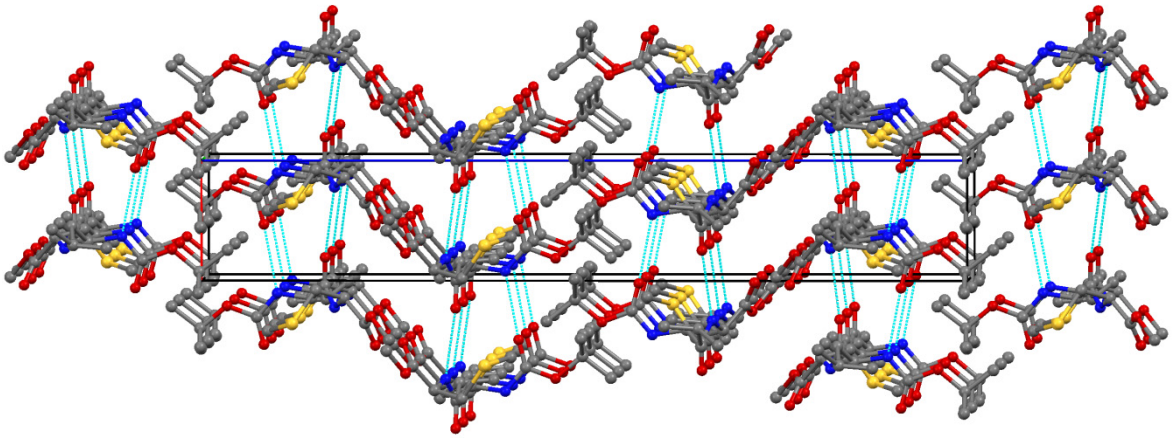

Figure S19. Overall packing of Boc-L-Leu-L-Cys(Me)-OMe as viewed nearly down the *b* axis. The intermolecular H-bonds are indicated by dashed lines.

HPLC-Mass Spectrometry

High-resolution mass spectra were obtained by electrospray ionization on a Perseptive Biosystem Mariner ESI-TOF spectrometer (Foster City, CA). An 1 x 10^{-9} M solution of neurotensin, angiotensin I, and bradykinin in an 1:1 CH_3CN/H_2O mixture, containing 1% formic acid, was used for calibration. The HPLC column used was Agilent Zorbax C18 0.1%. The mobile phase solvents are composed of A: 0.1% formic acid in water and B: 0.1 % formic acid in acetonitrile. The HPLC measurements were performed using an Agilent 1200 series apparatus (Palo Alto, CA). The Photo Diode array (PDA) was set to monitor UV scan from 200 to 450 nm and the chromagram was recorded at 275 nm. The HPLC-MS analysis of the Azo derivatives was carried out before and after the UV irradiation to investigate the catalytic process of the ***ternary catalyst***. Full scan mass spectra, in both positive and negative ion modes, were acquired over a mass scan range of 100-400 amu.

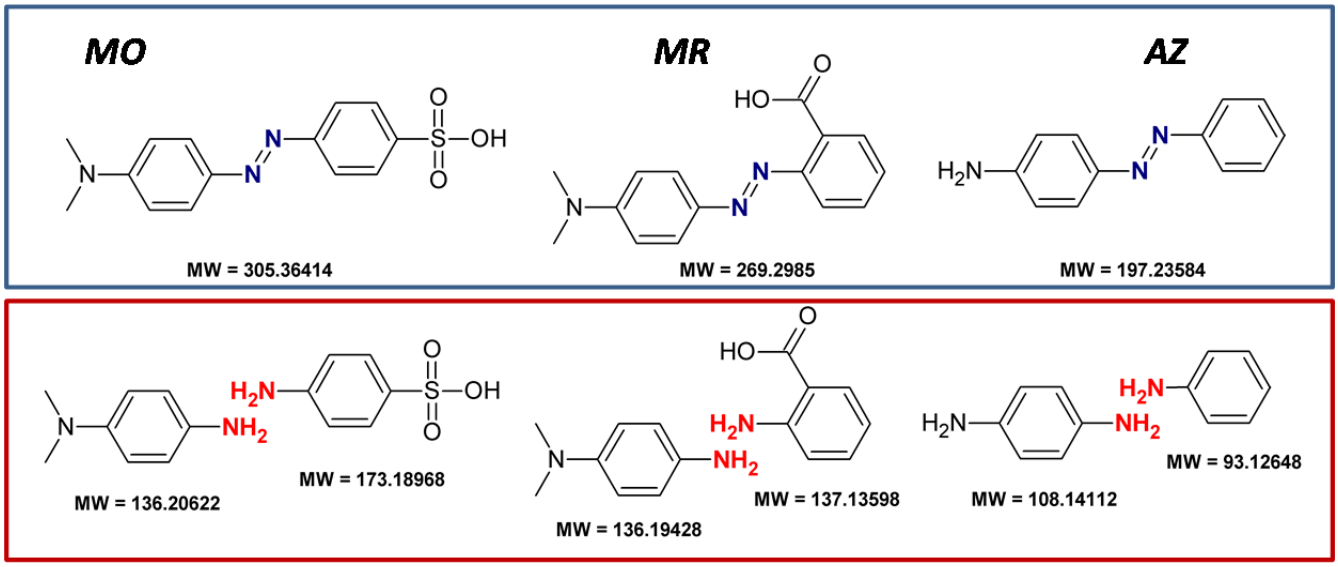

Characterization of the reduced species of Methyl Orange

The chromatographic separation of Methyl Orange (MO) run at 0, 20 and 45 and 60 min after UV irradiation respectively were monitored using full scan MS experiments. Before UV irradiation treatment the MS chromatograms of time 0 min sample showed only one chromatographic peak characterized by a molecular ion at *m/z* 306 $[M+H]^+$ corresponding to MO. After 20 min of UV irradiation, the chromatographic peak at *m/z* 306 decreased, and two new additional peaks were detected in the sample with different retention times. In particular one peak reveled a molecular ion at *m/z* 172 $[M-H]^-$ (attributed to a reduced specie of methyl orange with a formula of $C_6H_7NSO_3$), while the other peak reveled a a molecular ion at *m/z* 137 $[M+H]^+$ (attributed to the other reduced specie of methyl orange with a formula $C_8H_{12}N_2$). After 45 and 60 min of UV irradiation, in both samples, only the two molecular ions at *m/z* 137 $[M+H]^+$ and *m/z* 172 $[M-H]^-$ were detected. No other degradation products of MO were detected in the samples after UV irradiation.

Characterization of the reduced species of Methyl Red

The chromatographic separation of Methyl Red (MR) run at 0, 20 and 45 and 60 min after UV irradiation respectively, were monitored using full scan MS experiments. Before UV irradiation treatment the MS chromatograms of time 0 min sample showed only one chromatographic peak characterized by a molecular ion at *m/z* 270 $[M+H]^+$ corresponding to MR. After 20 min of UV irradiation, the chromatographic peak at *m/z* 270 decreased, and two new additional peaks were detected in the sample with different retention times. In particular one peak reveled a molecular ion at *m/z* 137 $[M+H]^+$ (attributed to a reduced specie of MR with a formula of $C_8H_{12}N_2$), while the other peak reveled a a molecular ion at *m/z* 138 $[M+H]^+$ (attributed to the other reduced specie of methyl orange with a formula $C_7H_7O_2N$). After 45 and 60 min of UV irradiation, in both samples, only the two molecular ions at *m/z* 137 $[M+H]^+$ and *m/z* 138 $[M+H]^+$ were detected. No other degradation products of MR were detected in the samples after UV irradiation.

Characterization of the reduced species of 4-amino-azobenzene

The chromatographic separation of 4-amino-azobenzene (AZ) run at 0, 20 and 45 and 60 min after UV irradiation respectively, were monitored using full scan MS experiments. Before UV irradiation treatment the MS chromatograms of time 0 min sample showed only one chromatographic peak characterized by a molecular ion at *m/z* 198 $[M+H]^+$ corresponding to MR. After 20 min of UV irradiation, the chromatographic peak at *m/z* 198 decreased, and two new additional peaks were detected in the sample with different retention times. In particular one peak reveled a molecular ion at *m/z* 94 $[M+H]^+$ (attributed to a reduced specie of MR with a formula of C_6H_7N), while the other peak reveled a a molecular ion at *m/z* 109 $[M+H]^+$ (attributed to the other reduced specie of methyl orange with a formula $C_6H_8N_2$). After 45 and 60 min of UV irradiation, in both samples, only the two molecular ions at *m/z* 94 $[M+H]^+$ and *m/z* 109 $[M+H]^+$ were detected. No other degradation products of MR were detected in the samples after UV irradiation.

Characterization of the reduced species of benzoic acid

The chromatographic separation of benzoic acid run at 0, 1, 2, 3 and 4 hours after UV irradiation respectively, were monitored using full scan MS experiments. Before UV irradiation treatment the MS chromatograms of time 0 min sample showed only one chromatographic peak characterized by a molecular ion at *m/z* 123 $[M+H]^+$ corresponding to benzoic acid. After 1 hour of UV irradiation, the chromatographic peak at *m/z* 123 decreased, and a new additional peaks were detected in the sample with different retention times. In particular the peak reveled a molecular ion at *m/z* 109 $[M+H]^+$ (attributed to a reduced specie of MR with a formula of C_6H_7N), while the other peak reveled a a molecular ion at *m/z* 109 $[M+H]^+$ (attributed to the other reduced specie of benzoic acid with a formula C_7H_8O). After 4 and hours of UV irradiation, only the two molecular ions at *m/z* 123 $[M+H]^+$ and *m/z* 109 $[M+H]^+$ were detected. From HPLC the ratio of reduction is 96%. No other degradation products of benzoic acid were detected in the samples after UV irradiation.